ACS Photonics

Letter

pubs.acs.org/journal/apchd5

High Thermo-Optic Coefficient of Silicon Oxycarbide Photonic Waveguides

Faisal Ahmed Memon,*[,†,‡] Francesco Morichetti,[†] and Andrea Melloni[†]

[†]Dipartimento di Elettronica, Informazione e Bioingegneria (DEIB), Politecnico di Milano, Via Ponzio 34/5, 20133 Milan, Italy

[‡]Department of Telecommunications Engineering, Mehran University of Engineering & Technology, Jamshoro 76062, Pakistan

ABSTRACT: In this Letter, we report on the observation of a high thermo-optic coefficient (TOC) of silicon oxycarbide (SiOC) films deposited by reactive RF magnetron sputtering for integrated photonic waveguides. In the 1550 nm wavelength range, the measured TOC of SiOC is as large as 2.5×10^{-4} RIU $°C^{-1}$, which is about 30 times larger than that of silica and almost twice that of silicon. Thin films of SiOC have been integrated in germanium-doped silica and silicon oxynitride conventional waveguide technology, achieving a 10× and 3× enhancement of the waveguide effective TOC, respectively. These results demonstrate the potential of SiOC for the realization of highly efficient phase actuators and low-power-consumption thermally tunable photonic integrated platforms.

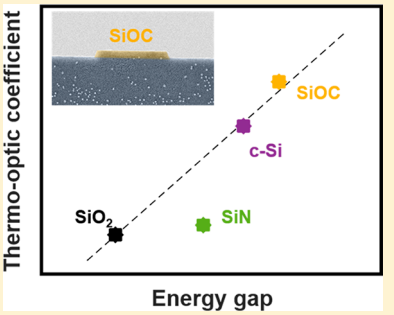

KEYWORDS: *integrated photonics, thermo-optic effect, silicon oxycarbide, optical waveguides*

Among the currently available integrated photonics platforms, dielectric technologies are the most consolidated, reliable, and widely exploited to realize commercial photonic integrated circuits (PICs). Conventional dielectric waveguide technologies include germanium-doped silica glass (Ge:SiO_2), silicon oxynitride (SiON), and silicon nitride (Si_3N_4).[1,2] These technologies have long been used to fulfill the requirements of photonic industries and enabled the fabrication of low-loss, low-cost, polarization-independent, efficient fiber-coupled, and relatively compact complex devices.

The tuning and reconfiguration of PICs is typically achieved through heaters that induce a phase shift in the propagating light by the thermo-optic effect. In dielectrics the thermo-optic coefficient dn/dT (TOC) is quite low, on the order of 10^{-5} $°C^{-1}$. On one hand, it can be seen as an advantage because it guarantees a weak dependence of PIC behavior on temperature variations; on the other hand, the efficiency of the heaters is rather low, as large electrical dissipation and large operational temperatures are required for control operations. Devices based on SiO_2, SiON, and Si_3N_4 show a spectral shift of about 1 GHz/°C, heaters are typically a few millimeters long, and the electrical power dissipated to induce a π phase shift is some hundreds of milliwatts. The high control temperatures introduce stringent requirements on the packaging and on the need of power-hungry Peltier cells to sink the heat. Further, the high temperatures on chip impact the reliability of the heaters, which deteriorate with time.

In order to realize energy-efficient and reliable reconfigurable PICs, materials with a large TOC could be integrated in conventional dielectric platforms. Examples of high-TOC materials employed in optical waveguides include silicon (1.8×10^{-4} $°C^{-1}$) and ultrarich silicon nitride (2.66×10^{-4} $°C^{-1}$).[3] High negative TOC values have been reported in polymers and TiO_2,[4] which are mainly related to the thermal expansion.

Silicon oxycarbide (SiOC) is a novel class of glass compounds that has gained momentum in the scientific community and adopted in technologically important applications such as interlayer dielectrics, anode material in lithium-ion batteries, and photoluminescence.[5−7] Recently, we have introduced SiOC as a potential platform in integrated photonics.[8,9] The refractive index of SiOC can be tailored from $n = 1.45$, corresponding to SiO_2, to about 3.2, for amorphous SiC.[10−12] SiOC has the advantage of a low absorption coefficient in the near-infrared region, and low-loss waveguides on silica realized by sputtering have been demonstrated for the first time with a core index of 1.578 and 2.2.[8,9] Waveguide attenuation of 2 to 4 dB/cm in the telecom window of 1550 nm has been measured. In comparison with SiON, exhibiting a pronounced absorption peak around 1505 nm due to N−H bonds,[1] SiOC absorption is spectrally flat across the full (S, C, L) telecom bands, offering a tremendous advantage for broadband applications.

In this Letter, we report on silica-buried SiOC channel waveguides where we observed a record TOC about 30 times larger than that of silica-based waveguides and even higher than that of silicon waveguides. Further, we propose and demonstrate the integration of SiOC films with classical dielectric waveguide technologies to enhance the efficiency of thermo-optic phase actuators. Results suggest that the high TOC of SiOC can be effectively exploited to achieve an energy-efficient reconfiguration of integrated photonic circuits based on conventional technologies such as Ge:SiO_2, SiON, SiN, and others.

Received: April 19, 2018
Published: June 15, 2018

DOI: 10.1021/acsphotonics.8b00512
ACS Photonics XXXX, XXX, XXX−XXX

The cross section of the silica-buried SiOC channel waveguide is shown in Figure 1a together with a scanning

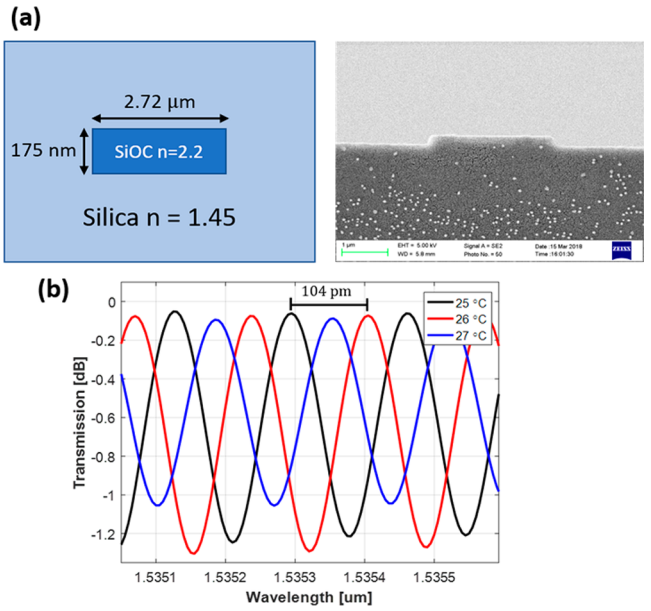

Figure 1. (a) Schematic and SEM photograph of the cross section of the SiOC channel waveguide. (b) Spectral response of a straight waveguide for three different temperatures.

electron microscopy (SEM) microphotograph of an uncovered waveguide. The SiOC core of the waveguide has a rectangular shape (2.72 × 0.175 μm^2) and a refractive index of 2.2. The SiOC film was deposited on a silicon wafer with a 6 μm thick silica substrate by using reactive radio frequency (RF) magnetron sputtering from a SiC target in an oxygen and argon atmosphere. Details on the SiOC sputtering procedure can be found in previous publications.[8,9] X-ray photoelectron spectroscopy (XPS) measurements revealed that the deposited material contain 45% silicon, 27% oxygen, and 27% carbon, so that the actual chemical composition is $Si_{0.45}O_{0.27}C_{0.27}$ (for brevity, in the remaining of the paper it will be simply referred to as SiOC omitting the subscripts). Good adhesion of the SiOC film on the silica substrate was observed, with no evidence of either pin holes or porosity. The SiOC surface roughness, as estimated with atomic force microscopy (AFM), is as low as 0.24 nm rms, which is comparable to the silica substrate. The optical constants of the SiOC film were measured with a variable-angle spectroscopic ellipsometer over a broad spectral range from the UV to near-infrared regions.[9] Around a wavelength of 1550 nm the measured refractive index of the SiOC layer is about 2.2 and the extinction coefficient is less than 10^{-4} above 600 nm.

The waveguide cross section was defined by direct-laser-writing lithography using an AZ 5214E photoresist and etching with a reactive ion etching (RIE) machine. The RIE process of mixed gases CHF_3 (100 sccm) and O_2 (5 sccm) was run applying an RF power of 50 W and inductively coupled plasma (ICP) power of 250 W for 20 min. The etch rate was 9 nm/min. After the SiOC core patterning, plasma enhanced chemical vapor deposition (PECVD) silica with n = 1.45 was deposited as the upper cladding material. The strip-shaped waveguide was selected in order to have good transverse electric (TE) mode properties, with a small contribution of the sidewall roughness to the waveguide attenuation. Several waveguides with different widths, ranging from 2 to 4 μm, were fabricated and tested. The waveguide propagation losses measured by cut-back technique are about 2 dB/cm.

The TOC of SiOC was estimated by optical transmission measurement of the fabricated waveguides at different temperatures. The photonic sample was mounted on a holder whose temperature was controlled by a thermoelectric Peltier module with a temperature accuracy within 0.1 °C. Lensed optical fibers were used to launch the light from a tunable laser, and the polarization state of light was controlled with a polarization controller guaranteeing at least −30 dB crosstalk between TE and transverse magnetic (TM) polarizations. TE-polarized light was coupled to the SiOC waveguides from a tunable laser operating in the broad spectral range from 1520 to 1580 nm.

Figure 1b shows the measured transmission spectrum of a SiOC waveguide around a wavelength λ = 1535.3 nm at three different temperatures. The Fabry−Pérot fringes due to the glass−air reflections at the waveguide input/output facets have a period $\Delta\lambda$ = 172 pm. The waveguide length is L = 3.5 mm and the effective group index results $n_g = \lambda^2/2L\Delta\lambda$ = 1.95. When the temperature is increased by 1 °C, for instance from 25 °C (black curve) to 26 °C (red curve), a wavelength shift of the waveguide transmission spectrum by $d\lambda/dT$ = 104 pm/°C is observed. The same wavelength shift was measured also from 26 to 27 °C (blue curve) and for any additional temperature degree. The effective thermo-optic coefficient of the waveguide, hereinafter referred to as K_{eff}, is given by

$$K_{\text{eff}} = \frac{n_g d\lambda}{\lambda dT} \tag{1}$$

and results to be K_{eff} = 1.34 × 10^{-4} °C^{-1}, a factor 10 larger than that of Si_3N_4 waveguides and 15 with respect to SiO_2-based waveguides.

The thermo-optic coefficient of the SiOC material can be evaluated by considering the overlap of the optical mode with all the materials the waveguide is made of. With a variational approach the perturbation of the phase propagation constant β due to a variation $\Delta\varepsilon(x, y)$ of the dielectric constant of the waveguide is given by[13,14]

$$P\Delta\beta = \omega \iint_A \Delta\varepsilon(x, y)\mathbf{E}\mathbf{E}^* \, dx \, dy \tag{2}$$

where **E** is the electric field of the guided mode, P is the power carried by the mode, and the integral is over the entire waveguide cross section A. Assuming that the perturbation is induced by a change of temperature dT, $\Delta\beta = \omega K_{eff} \, dT/c$ and, for each material, $\Delta\varepsilon = 2nK \, dT$, where K is the material TOC.

The effective thermo-optic coefficient K_{eff} can hence be written as a combination of the contribution of the various materials,

$$K_{\text{eff}} = \sum_i K_i \Gamma_i \tag{3}$$

where K_i is the thermo-optic coefficient of the ith material and

$$\Gamma_i = \frac{c \iint_{A_i} [\varepsilon o \vec{E} \cdot \vec{E}^*] \, dx \, dy}{\iint_A [\varepsilon o \vec{E}_t \times \vec{H}_t^*] \cdot \hat{z} \, dx \, dy} \tag{4}$$

is the confinement factor of the mode in the considered material, which is evaluated across a cross-sectional area A_i. From eq 3 and the measured value of K_{eff} of the waveguide, the

DOI: 10.1021/acsphotonics.8b00512
ACS Photonics XXXX, XXX, XXX−XXX

thermo-optic coefficient of the SiOC material is $K_{SiOC} = 2.5 \times 10^{-4}$ °C^{-1}, one of the largest values ever reported for dielectric materials. Table 1 reports the values of the confinement factor

Table 1. Materials and Waveguide Parameters

technology	SiOC wg	SiOC coated Ge:SiO_2 wg	SiOC coated SiON ring
group index n_g	1.95	1.93	1.574
index contrast	34%	1.5%	5.7%
size [μm^2]	2.72 × 0.175	3.5 × 2.8	2.5 × 1.8 × 0.4
$\Delta\lambda$ [pm]/°C	104	130	31.3
Γ_{SiO2}	0.59	0.59	0.26
Γ_{SiOC}	0.53	0.46	0.049
Γ_{SiON}			0.72
$K_{eff} \times 10^{-4}$ (expt)	1.34	1.62	0.32

in the SiOC ($\Gamma_{SiOC} = 0.53$) and SiO_2 ($\Gamma_{SiO2} = 0.589$) layers of the waveguide, as evaluated from electromagnetic simulations. The thermo-optic coefficient of silica is $K_{SiO2} = 0.9 \times 10^{-5}$ °C^{-1}.

The high TOC of SiOC, together with the transparency at telecom wavelengths and the high refractive index, suggests its use as a potential candidate for high integration scale and low control power integrated optics. Here, we propose and demonstrate the exploitation of SiOC for realizing highly efficient thermo-optic phase shifters in classical and well-consolidated photonic technologies, such as Ge-doped SiO_2 and SiON waveguides.

A thin layer of SiOC was deposited on the core of the optical waveguides, which was then buried under a PECVD silica upper cladding. The cross sections and micrographs of the SiOC-coated Ge:SiO_2 waveguide and SiON ring resonator are shown in Figure 2. The index contrast of the Ge:SiO_2 waveguide is 1.5%, and the core size is 3.5 × 2.8 μm^2; for the SiON waveguide, a rib shape with a size of 2.5 × 1.8 μm^2 (slab height of 0.4 μm) is used, the index contrast being equal to 5.7%. Waveguide data are summarized in Table 1, and

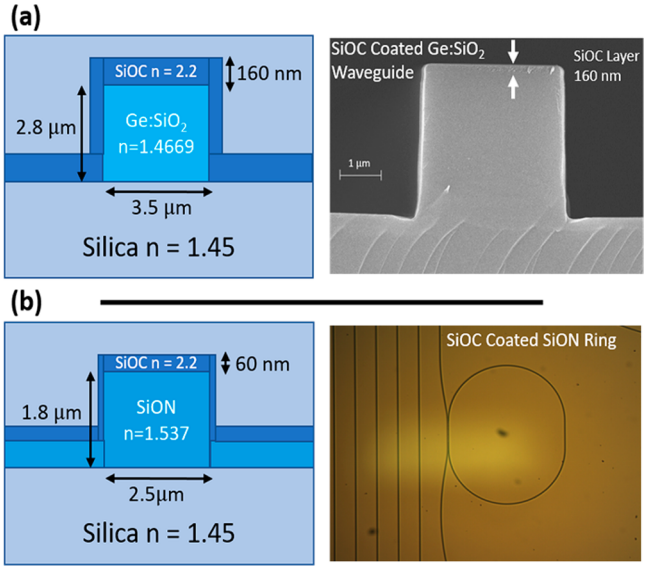

Figure 2. Cross section and microphotograph of (a) a Ge:SiO_2 waveguide coated with a SiOC layer; (b) a SiOC-coated SiON waveguide and ring resonator.

details of their respective fabrication and optical characterization can be found in specific contributions.[15,16] Electromagnetic simulations were performed to optimize the overlap of the guided mode with the SiOC layer and limit the perturbation on the waveguides. The thickness of the deposited SiOC layers is 160 and 60 nm for Ge:SiO_2 and SiON waveguiding structures, respectively. The thickness of the deposited SiOC films on the waveguide sidewalls is about 40% of the top SiOC layer thickness, as estimated from the SEM image given in Figure 2a.

Experiments were performed on Ge:SiO_2 straight waveguides and SiON ring resonators coated with the SiOC film. The radius of the ring resonator is 555.3 μm, the coupler length is 260 μm, and the physical length of the cavity is 4.009 mm. As in the case of the SiOC-core waveguide discussed in Figure 1, K_{eff} was estimated by optical transmission measurements of the fabricated structures at different temperatures. Figure 3a shows the measured optical transmission spectrum of

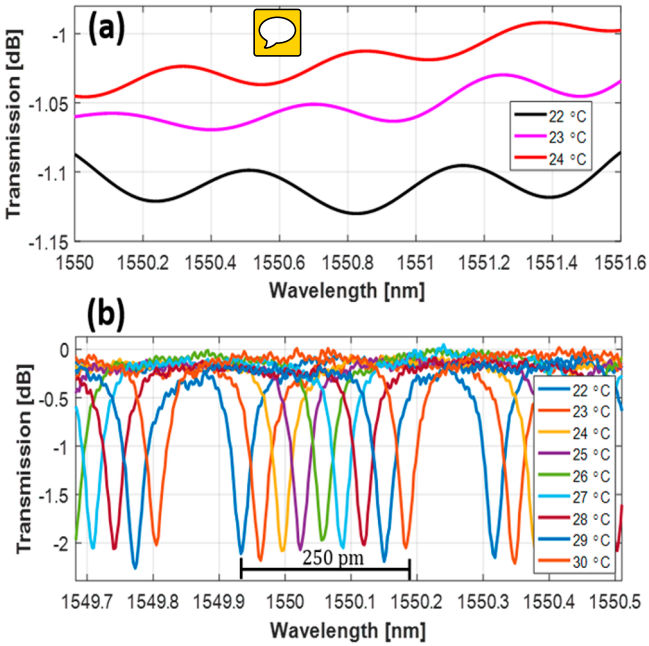

Figure 3. Spectral response of (a) a SiOC-coated Ge:SiO_2 straight waveguide for three different temperatures; (b) a SiOC-coated SiON ring resonator for nine different temperatures.

a SiOC-coated Ge:SiO_2 straight waveguide around $\lambda = 1550$ nm. The Fabry–Pérot fringes, which are less pronounced than in Figure 1(c) because of the lower effective index of the waveguide, reveal $n_g = 1.93$. When the temperature is increased by $dT = 1$ °C, a wavelength shift of the waveguide transmission spectrum $d\lambda/dT = 130$ pm/°C is observed. According to eq 1, this shift corresponds to an effective thermo-optic coefficient $K_{eff} = 1.62 \times 10^{-4}$ °C^{-1}, which is more than 1 order of magnitude higher than that of SiO_2 waveguides.

The enhancement of the waveguide effective TOC is confirmed by results achieved on SiOC-coated SiON waveguides. Figure 3b shows the thermally induced wavelength shift of the transmission spectrum of a microring resonator around a wavelength of 1550 nm. When the temperature increases from 22 °C to 30 °C, the resonance of the microring is shifted by 250 pm. From eq 1, the resulting K_{eff} is 3.2×10^{-5} °C^{-1}. Remarkably, a thin layer of SiOC of only 60 nm thickness and

DOI: 10.1021/acsphotonics.8b00512
ACS Photonics XXXX, XXX, XXX−XXX

with a confinement factor Γ_{SiOC} of less than 5% increases by 3 times the K_{eff} of the ring original SiON waveguides (K_{SiON} = 1.1 × 10^{-5} $°C^{-1}$). These results confirm that SiOC seems an enabling platform to develop highly efficient reconfigurable photonic systems.

The origin of the large TOC of SiOC is related to the volume change in polarizability and, in a minor part, on the thermal expansion. This is the typical situation for high melting point, high hardness, and high elastic moduli materials. Also, near the transparency edge, the polarizability (and dn/dT) rises.[17] Figure 4 reports the TOC of various materials plotted

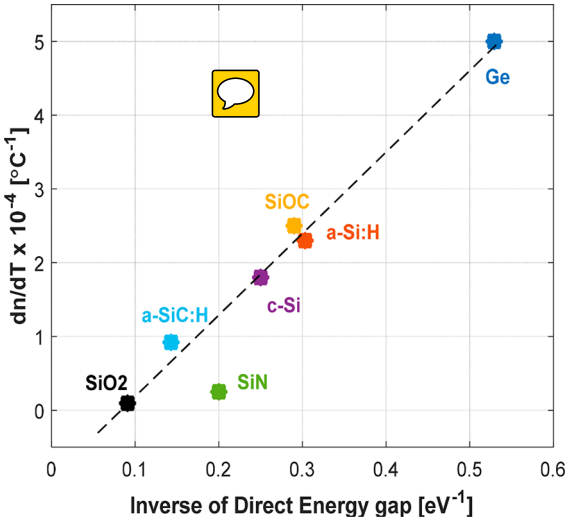

Figure 4. Thermo-optic coefficient dependence on the inverse of the direct band gap energy.

against their direct band gap energy E_g at telecom wavelengths. Reported data are obtained from the literature.[18,19] The thermo-optic coefficient is nearly dependent on the inverse of E_g and increases approaching the band gap. Silica is transparent until the deep UV and has a very small TOC, while germanium has the highest coefficient but it is not transparent at telecom wavelengths. The direct band gap of the SiOC film has been determined by using absorption spectra measured with spectroscopic ellipsometry and applying the Tauc relation $(\alpha h\omega)^2 = h\omega - E_g$, where α is the absorption coefficient and $h\omega$ is the photon energy.[20] The direct band gap of the SiOC film with n = 2.2 is calculated as E_g = 3.5 eV,[9] which is lower than that of Si and is responsible for its higher thermo-optic coefficient. As can be seen in Figure 4, SiOC is aligned with the trend of increasing TOC value with decreasing energy band gap.

In conclusion, we investigated the thermo-optic effect in optical waveguides integrating high refractive index (n = 2.2) SiOC films. Experiments on three different waveguiding structures (channel SiOC waveguide, SiOC-coated SiO_2 waveguide, and SiOC-coated SiON waveguide) show that the thermo-optic coefficient of SiOC, amounting to 2.5 × 10^{-4} $°C^{-1}$, is 1 order of magnitude larger than that of dielectric materials conventionally employed in integrated optics and almost twice that of silicon. The high TOC of SiOC was also exploited to achieve a significant enhancement of the TOC of conventional glass waveguides (10× in SiO_2, 3× in SiON waveguides) by coating the waveguide core with a thin film of SiOC. These results demonstrate the potential of SiOC for the realization of highly efficient thermally tunable photonic integrated platforms.

AUTHOR INFORMATION

Corresponding Author

*E-mail: faisalahmed.memon@polimi.it.

ORCID

Faisal Ahmed Memon: 0000-0002-4198-3694

Francesco Morichetti: 0000-0002-5858-2811

Author Contributions

F.A.M. fabricated the waveguides and performed experiments for the characterization of the thermo-optic coefficient of SiOC. Results were discussed by all authors. The manuscript was written and approved by all authors.

Notes

The authors declare no competing financial interest.

ACKNOWLEDGMENTS

This work was partially funded by Fondazione Cariplo Project "Advanced Control Technologies for Integrated Optics (ACTIO)", Rif. 2016-0881. F.A.M. acknowledges Erasmus Mundus LEADERS Project for the Ph.D. scholarship. The work was mainly performed at Polifab (www.polifab.polimi.it), the micro/nano fabrication facility at Politecnico di Milano, Italy.

REFERENCES

(1) de Ridder, R. M.; Worhoff, K.; Driessen, A.; Lambeck, P. V.; Albers, H. Silicon oxynitride planar waveguiding structures for application in optical communication. *IEEE J. Sel. Top. Quantum Electron.* **1998**, *4*, 930.

(2) Muñoz, P.; Micó, G.; Bru, L. A.; Pastor, D.; Pérez, D.; Doménech, J. D.; Fernández, J.; Baños, R.; Gargallo, B.; Alemany, R.; Sánchez, A. M.; Cirera, J. M.; Mas, R.; Domínguez, C. Silicon Nitride Photonic Integration Platforms for Visible, Near-Infrared and Mid-Infrared Applications. *Sensors* **2017**, *17*, 2088.

(3) Lim, K. P.; Krishnamurthy, V.; Ying, J. F.; Pu, J.; Wang, Q. Ultrahigh index and low-loss silicon rich nitride thin film for NIR HAMR optics. *IEEE Trans. Magn.* **2017**, *53* (5), 1–7.

(4) Bovington, J.; Wu, R.; Cheng, K.-T.; Bowers, J. E. Thermal stress implications in athermal TiO_2 waveguides on a silicon substrate. *Opt. Express* **2014**, *22*, 661–666.

(5) Mandracci, P.; Frascella, F.; Rizzo, R.; Virga, A.; Rivolo, P.; Descrovi, E.; Giorgis, F. Optical and structural properties of amorphous silicon-nitrides and silicon-oxycarbides: Application of multilayer structures for the coupling of Bloch Surface Waves. *J. Non-Cryst. Solids* **2016**, *453*, 113–117.

(6) David, L.; Bhandavat, R.; Barrera, U.; Singh, G. Silicon oxycarbide glass-graphene composite paper electrode for long-cycle lithium-ion batteries. *Nat. Commun.* **2016**, *7*, 10998.

(7) Nikas, V.; Gallis, S.; Huang, M.; Kaloyeros, A. E.; Nguyen, A. P. D.; Stesmans, A.; Afanas'ev, V. V. The origin of white luminescence from silicon oxycarbide thin films. *Appl. Phys. Lett.* **2014**, *104*, 061906.

(8) Memon, F. A.; Morichetti, F.; Melloni, A. Waveguiding light into silicon oxycarbide. *Appl. Sci.* **2017**, *7* (6), 561.

(9) Memon, F. A.; Morichetti, F.; Melloni, A. Integrated photonic devices with silicon oxycarbide. *SPIE Photonics Europe Conference* **2018**, 125.

(10) Ryan, J. V.; Pantano, C. G. Synthesis and characterization of inorganic silicon oxycarbide glass thin films by reactive rf-magnetron sputtering. *J. Vac. Sci. Technol., A* **2007**, *25* (1), 153–159.

(11) Miyazaki, H. Structure and optical properties of silicon oxycarbide films deposited by reactive RF magnetron sputtering using a SiC target. *Japanese J. of Appl. Physics* **2008**, *47* (11R), 8287.

DOI: 10.1021/acsphotonics.8b00512
ACS Photonics XXXX, XXX, XXX–XXX

(12) Du, P.; Wang, X.; Lin, I. K.; Zhang, X. Effects of composition and thermal annealing on the mechanical properties of silicon oxycarbide films. *Sens. Actuators, A* **2012**, *176*, 90−98.
(13) Tamir, T. *Guided-Wave Optoelectronics*; Springer, 1988.
(14) Robinson, J. T.; Preston, K.; Painter, O.; Lipson, M. First-principle derivation of gain in high-index-contrast waveguides. *Opt. Express* **2008**, *16*, 16659−16669.
(15) Melloni, A.; Costa, R.; Monguzzi, P.; Martinelli, M. Ring-resonator filters in silicon oxynitride technology for dense wavelength-division multiplexing systems. *Opt. Lett.* **2003**, *28*, 1567−1569.
(16) http://www.enablence.com/technologies/.
(17) Bass, M. *Handbook of Optics: Vol. IV - Optical Properties of Materials, Nonlinear Optics, Quantum Optics*; McGraw-Hill, 2010.
(18) Palik, E. D. *Handbook of Thermo-optic Coefficients of Optical Materials with Applications*; Academic, 1998.
(19) Della Corte, F. G.; Montefusco, M. E.; Moretti, L.; Rendina, I. Study of the thermo-optic effect in hydrogenated amorphous silicon and hydrogenated amorphous silicon carbide between 300 and 500 K at 1.55 μm. *Appl. Phys. Lett.* **2001**, *79*, 168.
(20) Tauc, J. Optical properties and electronic structure of amorphous Ge and Si. *Mater. Res. Bull.* **1968**, *3*, 37−46.

DOI: 10.1021/acsphotonics.8b00512
ACS Photonics XXXX, XXX, XXX−XXX